DOI: 10.1002/ejic.200601148

# The Relationship Between $^{27}Al$ Quadrupolar Parameters and $AlF_6^{3-}$ Octahedron Connectivity in Crystalline and Glassy Fluoroaluminates

**Monique Body,*[a] Christophe Legein,[b] Jean-Yves Buzaré,[a] and Gilles Silly[c]**

*This paper is dedicated to Professor Neil Bartlett on the occasion of his 75th birthday*

**Keywords:** Glasses / Fluorides / $^{27}Al$ NMR spectroscopy / Quadrupolar parameters

$^{27}Al$ SATRAS and MQ-MAS spectra were recorded for eight crystalline compounds, from the $CaF_2$–$AlF_3$ and $BaF_2$–$AlF_3$ binary and $BaF_2$–$CaF_2$–$AlF_3$ ternary systems, and four glass compositions with different $CaF_2$/$BaF_2$/$AlF_3$ contents. For the crystalline phases, the reconstruction of the spectra leads to the precise determination of the NMR parameters. For the glassy phases, the $^{27}Al$ SATRAS spectra have been reconstructed using quadrupolar parameter distributions. The main finding of this study is the dependence of the quadrupolar frequency on the type of $AlF_6^{3-}$ octahedron connectivity. For crystalline phases the experimental $\nu_Q$ values range between 75 kHz and 510 kHz for structures built up from isolated octahedra, and are between 560 kHz and 1250 kHz for structures built up from isolated chains of *cis*-connected octahedra, and are between 1530 kHz and 1580 kHz for structures built up from isolated chains of *trans*-connected octahedra. In the glassy phases the maximum of the quadrupolar frequency distribution shifts toward larger values and its width increases with increasing $AlF_3$ content, and subsequently with the number of connected octahedra. The range of the $\nu_Q$ values seems to indicate that when the octahedra are connected, *cis* connections occur most frequently.


## Introduction

The use of $^{27}Al$ NMR can provide important structural information relating to the local order around aluminium atoms in crystalline and disordered compounds. Numerous $^{27}Al$ NMR studies have been performed on a wide range of chemical systems. Oxide minerals have been particularly well studied. The isotropic chemical shifts observed in the spectra for these materials have been used to determine the nature of the Al coordination, and for obtaining information about the chemical environments of the Al atoms.

As aluminium atoms have a quadrupolar nucleus ($I$ = 5/2), other valuable structural information may also be obtained through the quadrupolar interactions. Actually, the $^{27}Al$ NMR spectra are broadened by this interaction even under Magic Angle Spinning (MAS) conditions. This hinders the precise determination of the quadrupolar parameters, especially when several crystallographically independent Al sites are present in the compound. However, the development of techniques such as SAtellite TRAnsition Spectroscopy (SATRAS),[1,2] and Multiple Quantum Magic Angle Spinning (MQ-MAS),[3] which are able to average first- and second-order broadenings, have allowed high-resolution $^{27}Al$ NMR spectra to be recorded from which the quadrupolar parameters in crystalline compounds,[4–20] and their distributions in disordered phases,[16,21–30] can be accurately determined.

In this paper we present a $^{27}Al$ NMR study of crystalline and glassy fluoride phases that are built up from $AlF_6^{3-}$ octahedra. The compounds under investigation are crystalline fluoridoaluminates of the $BaF_2$–$AlF_3$ (α-, β- and γ-$BaAlF_5$, $Ba_3Al_2F_{12}$, and $Ba_3AlF_9$-Ib) and $CaF_2$–$AlF_3$ binary systems (α-$CaAlF_5$, $Ca_2AlF_7$), α-$BaCaAlF_7$, and glassy phases of the corresponding $BaF_2$–$CaF_2$–$AlF_3$ ternary system ($50CaF_2$–$15BaF_2$–$35AlF_3$, $35CaF_2$–$25BaF_2$–$40AlF_3$, $35CaF_2$–$20BaF_2$–$45AlF_3$, and $35CaF_2$–$15BaF_2$-$50AlF_3$). We have already investigated β-$CaAlF_5$ and β-$Ba_3AlF_9$ by $^{27}Al$ NMR spectroscopy.[18,19] The crystalline compounds belonging to these systems that are not included in this study are as follows: $Ba_5AlF_{13}$ and $Ba_5Al_3F_{19}$, the crystal structures of which are unknown,[31] δ-$BaAlF_5$[32] which, to the best of our knowledge, cannot

[a] Laboratoire de Physique de l'Etat Condensé, CNRS UMR 6087, Institut de Recherche en Ingénierie Moléculaire et Matériaux Fonctionnels, CNRS FR 2575, Université du Maine, Avenue Olivier Messiaen, 72085 Le Mans Cedex 9, France
Fax: +33-2-43833518
E-mail: monique.body@univ-lemans.fr
[b] Laboratoire des Oxydes et Fluorures, CNRS UMR 6010, Institut de Recherche en Ingénierie Moléculaire et Matériaux Fonctionnels, CNRS FR 2575, Université du Maine, Avenue Olivier Messiaen, 72085 Le Mans Cedex 9, France
[c] Laboratoire de Physicochimie de la Matière Condensée, CNRS UMR 5617, Institut Charles Gerhardt, CNRS FR 1878, Université de Montpellier II, Place Eugène Bataillon, C.C. 03, 34095 Montpellier Cedex 5, France

   

be obtained by a solid-state reaction, and $Ba_3AlF_9$-Ia, which we were unable to synthesize.[33] SATRAS experiments were carried out for all the studied samples. For multi-site crystalline phases and glasses, MQ-MAS spectra were also recorded. The reconstruction of the NMR spectra leads to the determination of the quadrupolar parameters for the crystalline compounds. These quadrupolar parameters are then classified according to the $AlF_6^{3-}$ octahedron connectivities.

The reconstructions of the SATRAS spectra for the $BaF_2$–$CaF_2$–$AlF_3$ glassy phases lead to a determination of the quadrupolar parameter distributions in relation to the $AlF_3$ content. These results are discussed in the light of a recent $^{19}$F NMR study on the same glassy phases,[34] which led to the experimental determination of the mean number, $\beta$, of fluorine atoms per $AlF_6^{3-}$ octahedron. It was shown that the $\beta$ value is between 6 and 5 for the studied glasses, and is dependent on the amount of $AlF_3$ in the glass (35–50%). For $\beta$ = 6, the $AlF_6^{3-}$ octahedra are isolated, and $\beta$ = 5 may correspond to the presence of infinite chains of octahedra in the glass. Correlation of $^{27}$Al NMR results for glassy and crystalline phases with $^{19}$F NMR spectroscopic data analyses of the glassy phases enables an accurate picture to be gained of the glass network through the dependence of the quadrupolar parameters on the octahedron connectivity.

## Results

### $^{27}$Al Quadrupolar Parameters in Crystalline Compounds

All the compounds under investigation are built up from a framework of $AlF_6^{3-}$ octahedra. In α- and β-$CaAlF_5$[35,18] only infinite isolated chains of $AlF_6^{3-}$ octahedra sharing *trans*-fluorine atoms are present, as shown in Figure 1a. The chains are corrugated, and the F–Al–F angles are equal to 157.5° and 155.8° in α- and β-$CaAlF_5$, respectively. In α-,[36] β-, and γ-$BaAlF_5$[37], the octahedra share corners at the *cis* position to form infinite isolated chains as shown in Figure 1b. The Al–F–Al angles show small variations: 146.2° in α-$BaAlF_5$, 145.9° and 145.6° in β-$BaAlF_5$, and 144.5° and 139.5° in γ-$BaAlF_5$.

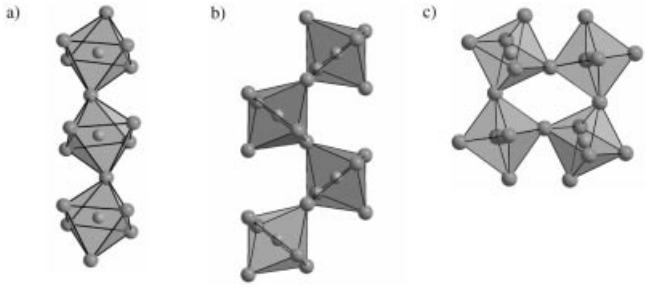


Figure 1. The different connectivities of the $AlF_6^{3-}$ octahedra encountered in the investigated crystalline phases: isolated chains of (a) *trans*-connected octahedra, (b) *cis*-connected octahedra and (c) tetrameric group of *cis*-connected octahedra.

There is only one unique aluminium site present in the α-$CaAlF_5$[35] and α-$BaAlF_5$[36] structures. Accordingly, for both compounds, the central transitions of the SATRAS spectra (Figure 2) correspond to one Al site. These central transitions present singularities that are characteristic of high quadrupolar frequency values. However, the line shape of the α-$CaAlF_5$ central transition is typical of an $\eta_Q$ value that is nearly equal to 1, whereas the central transition in the α-$BaAlF_5$ spectrum corresponds to a small $\eta_Q$ value. The method for extracting the NMR parameters has been described in detail for β-$CaAlF_5$;[16] an initial estimation of the quadrupolar parameters $\nu_Q$ and $\eta_Q$ is obtained from the reconstruction of the central transition line shape (Figure 2), and then precise values are given by the reconstruction of the overall spinning sideband envelope shape. $AlF_3$ is present as an impurity in α-$CaAlF_5$ and its contribution has been included in the reconstructed spectrum with a relative intensity of 0.5%, using the relevant NMR parameters previously determined by Silly et al.[15]. The NMR parameters leading to the best simulations are summarized in Table 1. $^{27}$Al MAS NMR spectra were previously recorded by Sakida et al.[38] for α-$CaAlF_5$ and α-$BaAlF_5$. However, these authors did not determine the quadrupolar parameter values, and they did not give the $\delta_{iso}$ value for α-$CaAlF_5$. However, they found $\delta_{iso}$ = –13.4 ppm for α-$BaAlF_5$, which is significantly different from our value. Their value is questionable since the experimental spectrum was not recon-

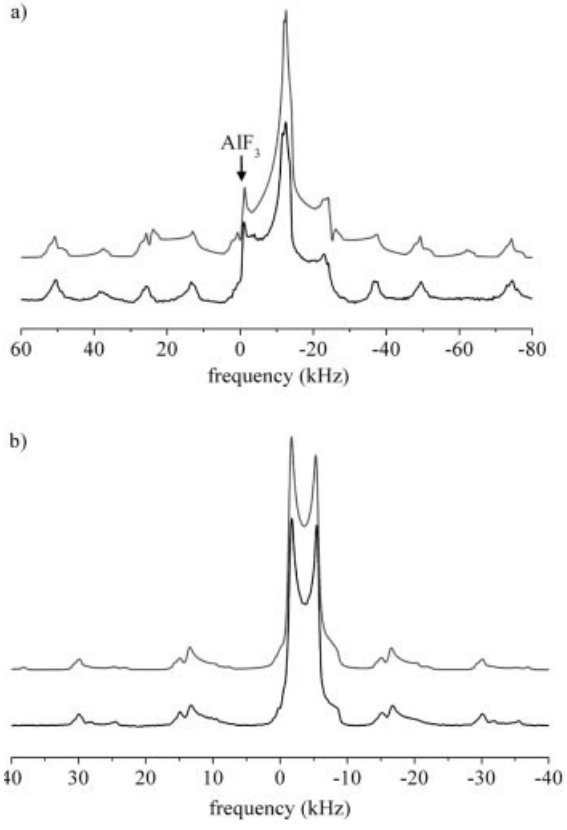


Figure 2. Experimental (bottom) and reconstructed (top) central transitions in the $^{27}$Al SATRAS NMR spectra for (a) α-$CaAlF_5$ (25 kHz) and (b) α-$BaAlF_5$ (15 kHz).

  

structed. We suggest that our results are more reliable as the experimental spectra were reconstructed taking into account all the interactions up to the second order.

Table 1. $AlF_6^{3-}$ octahedron connections, compounds, isotropic chemical shifts, $\delta_{iso}$ (ppm), quadrupolar frequencies, $\nu_Q$ (kHz), and asymmetry parameters, $\eta_Q$, from the reconstructions of the $^{27}Al$ NMR spectra.

| Connection | Compound | $\delta_{iso}$ (± 2) | $\nu_Q$ (± 5%) | $\eta_Q$ (± 0.05) |
|---|---|---|---|---|
| *trans* | α-$CaAlF_5$ | –6 | 1580 | 0.95 |
| | β-$CaAlF_5$[a] | –7 | 1530 | 0.10 |
| *cis* | α-$BaAlF_5$ | –3 | 1000 | 0.09 |
| | β-$BaAlF_5$ | –0.5 | 750 | 0.10 |
| | | –2 | 550 | 0.45 |
| | γ-$BaAlF_5$ | 1 | 1250 | 0.15 |
| | | –3 | 900 | 0.15 |
| | $Ba_3Al_2F_{12}$ | –2 | 560 | 0.30 |
| Isolated | $Ca_2AlF_7$ | –6 | 340 | 0.95 |
| | $Ba_3AlF_9$-Ib | 0 | 75 | 0.50 |
| | | 0 | 510 | 0.07 |
| | β-$Ba_3AlF_9$[b] | 1 | 140 | 0.50 |
| | | –2 | 210 | 0.85 |
| | α-$BaCaAlF_7$ | –0.5 | 190 | 0.80 |

[a] From ref.[18] [b] From ref.[19]

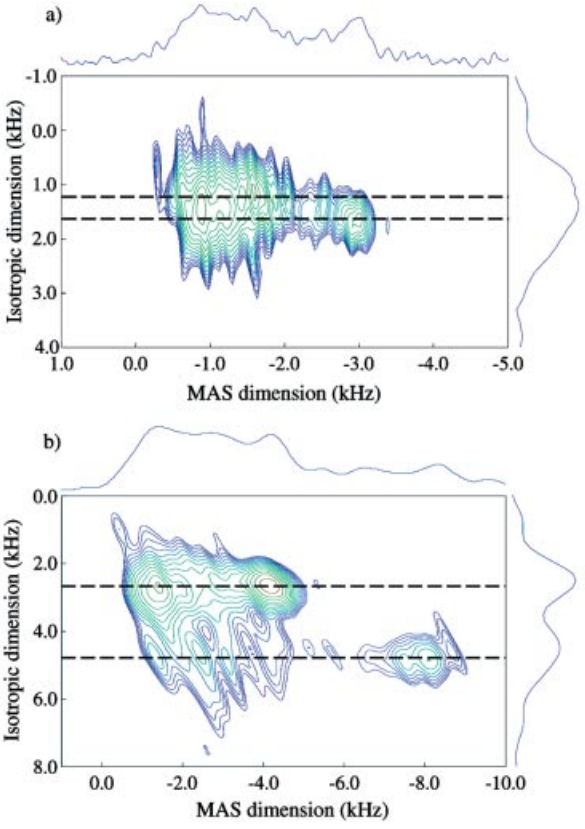


Figure 3. Experimental $^{27}Al$ 3Q-MAS NMR spectra for (a) β-$BaAlF_5$ and (b) γ-$BaAlF_5$ at 25 kHz. The curves at the top and to the right of the spectra are the projections of the spectra on to the MAS (*F2*) and isotropic (*F1*) axes, respectively. The dashed lines indicate the *F1* slices used for preliminary estimation of the NMR parameters.

Both the β- and γ-$BaAlF_5$ structures contain two symmetry-independent aluminium sites.[37] For these two compounds two aluminium sites can be resolved along the *F1* dimension in the 3Q-MAS spectra, as shown in Figure 3. As previously done for β-$Ba_3AlF_9$,[19] an initial estimation of the NMR parameters is given by the reconstruction of the *F1* slices. Then a precise determination of the NMR parameters is obtained from the reconstruction of the whole $^{27}Al$ SATRAS spectra. Two contributions of equal intensity are needed for the reconstruction of the β-$BaAlF_5$ SATRAS spectrum. Similarly, the two contributions used for the reconstruction of the γ-$BaAlF_5$ SATRAS spectrum have the same relative intensity. For both compounds the corresponding NMR parameters are listed in Table 1. The experimental and reconstructed central transitions are presented in Figure 4. In both compounds the Al sites have the same multiplicities, therefore ab initio calculations are required before any of these parameters can be attributed to the symmetry-independent Al atoms.

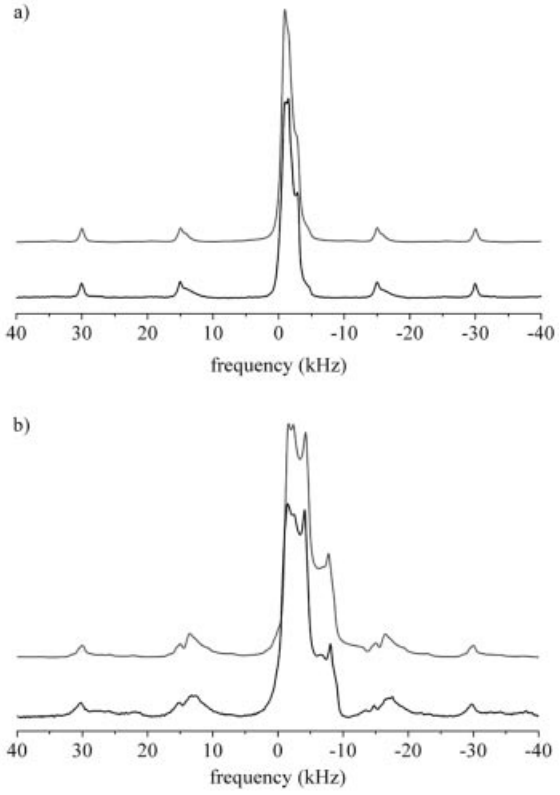


Figure 4. Experimental (bottom) and reconstructed (top) central transitions of the $^{27}Al$ SATRAS NMR spectra for (a) β-$BaAlF_5$ and (b) γ-$BaAlF_5$ at 15 kHz.

$Ba_3Al_2F_{12}$ comprises tetramers formed by four $AlF_6^{3-}$ octahedra sharing corners at the *cis* position,[39,40] as shown in Figure 1c. These tetrameric groups are separated from each other by barium and "free" fluorine ions (i.e. not linked to Al). Similarly, the NMR parameters were determined by first reconstructing the central transition, and then the whole experimental $^{27}Al$ SATRAS spectrum. These NMR parameters are given in Table 1. Experimental and reconstructed central transition and SATRAS spectra

  

are presented in Figure 5. Sakida et al.[38] determined an isotropic chemical shift value of $\delta_{iso}$ = –11.7 ppm for this compound. The comments made above with respect to α-$BaAlF_5$ hold for this compound as well.

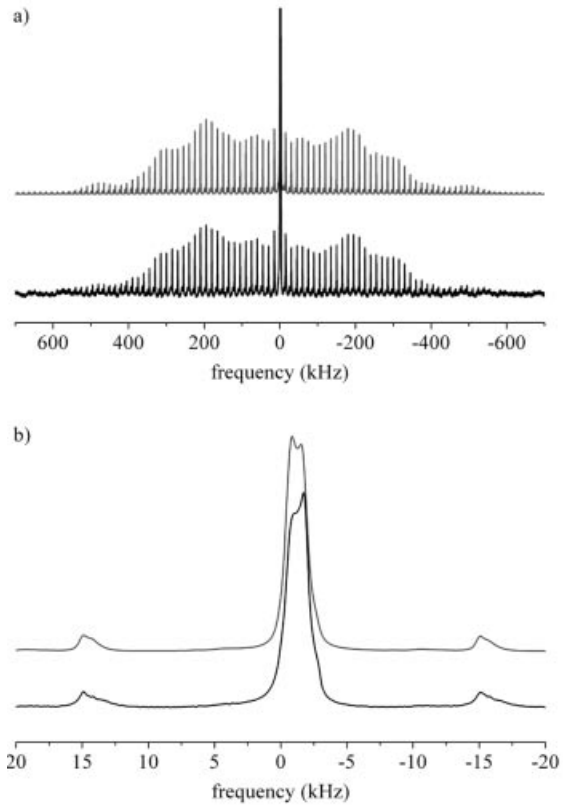


Figure 5. Experimental (bottom) and reconstructed (top) spectra: (a) $^{27}$Al SATRAS NMR spectra and (b) central transitions for $Ba_3Al_2F_{12}$ at 15 kHz. In the full SATRAS spectra the central transitions are truncated to improve the visiblity of the spinning sidebands.

$Ca_2AlF_7$,[41] $Ba_3AlF_9$-Ib,[42] β-$Ba_3AlF_9$,[43] and α-$BaCaAlF_7$[44] contain isolated $AlF_6^{3-}$ octahedra. $Ba_3AlF_9$-Ib and β-$Ba_3AlF_9$ are structurally quite different, even though they are both characterized by isolated $AlF_6^{3-}$ octahedra and $FBa_4^{7+}$ tetrahedra. β-$Ba_3AlF_9$ contains three aluminium sites; their corresponding NMR parameters have already been determined, and are reported in ref.[19] $Ca_2AlF_7$, $Ba_3AlF_9$-Ib, and α-$BaCaAlF_7$ contain one aluminium site, as confirmed by the $^{27}$Al SATRAS spectra presented in Figure 6. For these three spectra the central transitions are shapeless, and are therefore not shown. The shapeless central transitions, and the overall SATRAS spectrum expansions, may be related to low quadrupolar frequencies. The comparison between these three spectra indicates that $Ca_2AlF_7$ has the highest quadrupolar frequency, whereas $Ba_3AlF_9$-Ib has the lowest value. The NMR parameters leading to the best simulations are provided in Table 1. The $^{27}$Al MAS NMR spectrum of $Ca_2AlF_7$ previously recorded by Sakida et al.[38] presents two "split peaks" that we do not observe in our SATRAS spectrum.

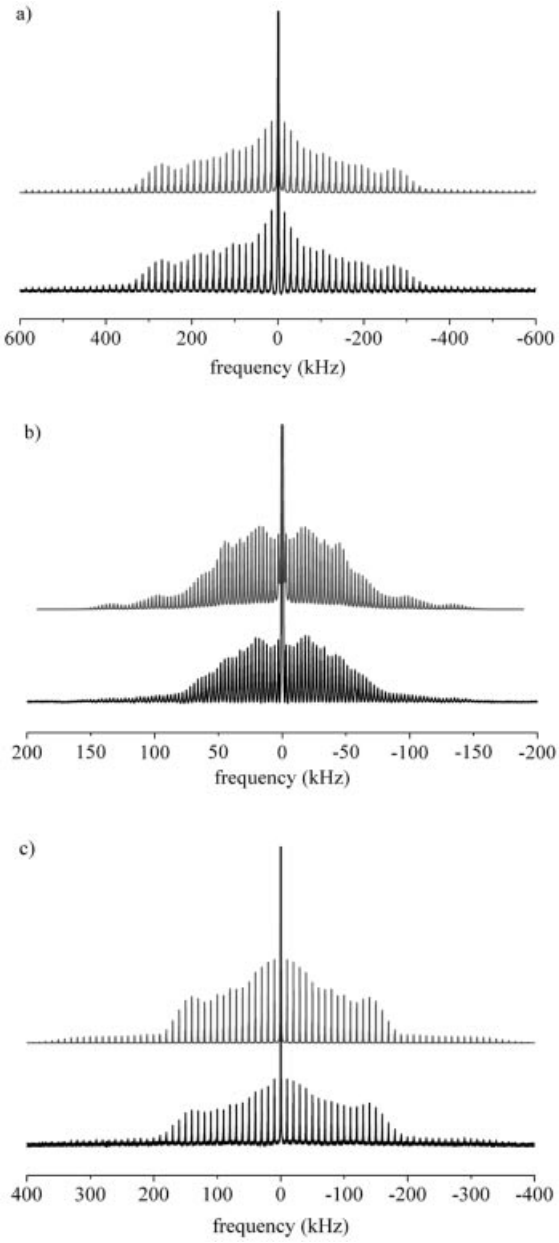


Figure 6. Experimental (bottom) and reconstructed (top) $^{27}$Al SATRAS NMR spectra for (a) $Ca_2AlF_7$ (15 kHz), (b) $Ba_3AlF_9$-Ib (3 kHz) and (c) α-$BaCaAlF_7$ (10 kHz). The central transitions are truncated to improve the visiblity of the spinning sidebands.

The previously published results for β-$CaAlF_5$[16] and β-$Ba_3AlF_9$[19] have been added to Table 1.

## Quadrupolar Parameters in Glassy Phases

For the $BaF_2$–$CaF_2$–$AlF_3$ ternary system several glass compositions have been synthesized in a previous study.[34] Four of these compositions have been chosen for this study, and contain 35–50% $AlF_3$. The selected glass compositions are given in Table 2.

  

Table 2. Glass compositions (mol fractions), isotropic chemical shifts, $\delta_{iso}$ (ppm), $\sigma$ parameters (kHz), and $\beta$ parameters for the studied glasses.

| Composition | $\delta_{iso}$ (± 2) | $\sigma$ (±20) | $\beta$[a] |
|---|---|---|---|
| $50CaF_2$–$15BaF_2$–$35AlF_3$ | –3 | 370 | 6 |
| $35CaF_2$–$25BaF_2$–$40AlF_3$ | –4 | 420 | 5.76 |
| $35CaF_2$–$20BaF_2$–$45AlF_3$ | –3 | 440 | 5.44 |
| $35CaF_2$–$15BaF_2$–$50AlF_3$ | –7 | 470 | 5 |

[a] From ref.[34]

The $^{27}$Al 3Q-MAS spectra clearly show only one Al contribution, and are presented in Figure 7. These spectra are similar to the those reported by Chan and Eckert for a related glass composition.[45] A striking feature of the data is the broadening of the 3Q-MAS spectra, which is expected to mirror the broadening of the quadrupolar parameter distribution with increasing $AlF_3$ glass content.

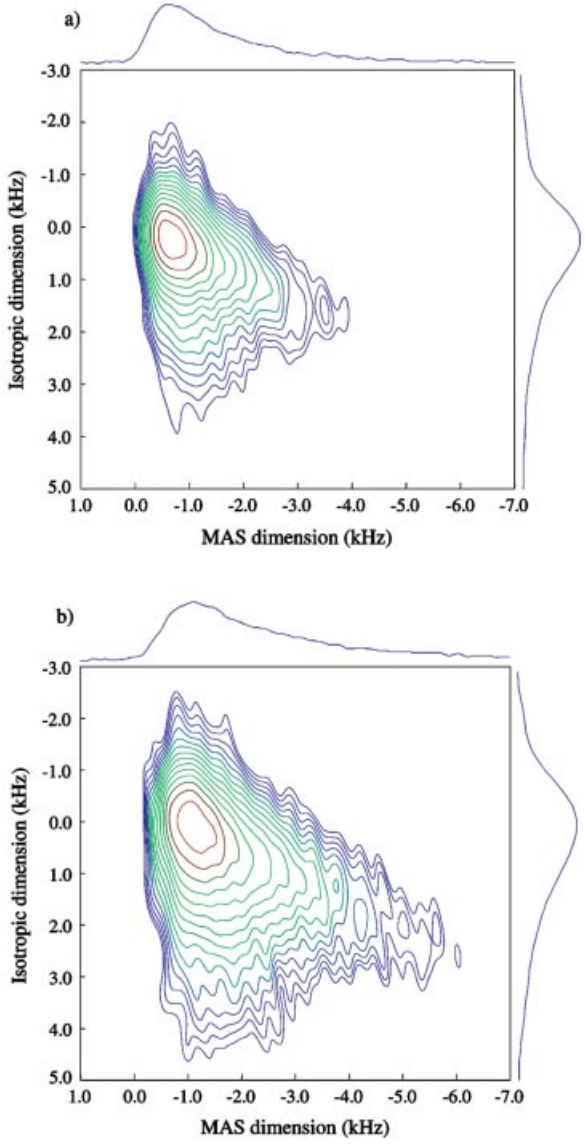


Figure 7. Experimental $^{27}$Al 3Q-MAS NMR spectra for (a) $50CaF_2$–$15BaF_2$–$35AlF_3$ and (b) $35CaF_2$–$15BaF_2$–$50AlF_3$ glasses at 25 kHz. The curves at the top and to the right of the spectra are the projections of the spectra on to the MAS (*F2*) and isotropic (*F1*) axes, respectively.

The $^{27}$Al SATRAS spectra, shown in Figure 8, were reconstructed using the Czjzek-like distribution[46,47] of the electric field gradients (EFG) [Equation (1)], where $\nu_Q = [3eQV_{zz}]/[2I(2I-1)h]$, $\eta_Q = [V_{xx} - V_{yy}]/V_{zz}$, $Q$ is the nuclear quadrupole moment, and $V_{ii}$ are the principal elements of the EFG tensor defined as $|V_{zz}| \geq |V_{yy}| \geq |V_{xx}|$.

$$P(\nu_Q, \eta_Q) = \frac{1}{\sqrt{2\pi}\sigma^d} \nu_Q^{d-1} \cdot \eta_Q \left(1 - \frac{\eta_Q^2}{9}\right) \cdot \exp\left(-\frac{\nu_Q^2\left(1 + \frac{\eta_Q^2}{3}\right)}{2\sigma^2}\right) \quad (1)$$

In Equation (1), $\sigma$ and $d$ are two adjustable parameters. The parameter $\sigma$ characterizes the strength of the quadrupolar interaction. When the five components of the quadrupolar tensor are independent, $d = 5$. In this case the distribution corresponds to the Gaussian Isotropic Model[48] in which the electric field gradient (EFG) distribution is assumed to correspond to statistical disorder.[28] Values of $d < 5$ account for local geometrical constraints.[47] Several tests have been performed for different $d$ values while assuming a unique value of the isotropic chemical shift. The best agreements between the experimental and reconstructed spectra were obtained with $d = 3$ and a line width equal to 350 Hz. This $d$ value is in agreement with previous studies on disordered and glassy aluminium and gallium phases, where good reconstructions of the $^{27}$Al and $^{69,71}$Ga NMR spectra were obtained with $d = 3$ corresponding to the metal atoms residing in octahedral environments.[26,49–51] The relevant parameters ($\delta_{iso}$, and $\sigma$) are given in Table 2. The $\delta_{iso}$ values are within the same range observed for the crystalline compounds, i.e. between –7 ppm and –2 ppm. The experimental and reconstructed $^{27}$Al SATRAS spectra for the glasses with lowest and highest $AlF_3$ contents are compared in Figure 8. The asymmetry of the central transitions is satisfactorily reproduced. The corresponding distributions $P(\nu_Q, \eta_Q)$ used for the reconstruction of these two spectra are shown in Figure 9. Most $\nu_Q$ values are within the range of 100–900 kHz for the 35% $AlF_3$ glass composition ($\sigma$ = 370 kHz and $d$ = 3), with a maximum around 450 kHz. For the 50% $AlF_3$ glass composition ($\sigma$ = 470 kHz and $d$ = 3), the distribution is enlarged, and most of the $\nu_Q$ values are between 100 kHz and 1200 kHz, with a maximum around 600 kHz. Moreover, these quadrupolar parameter distributions are nil when $\nu_Q$ and/or $\eta_Q$ are equal to zero. Therefore, high symmetrical EFGs are prohibited, as would be expected for materials exhibiting the level of disorder present in glassy phases.

  

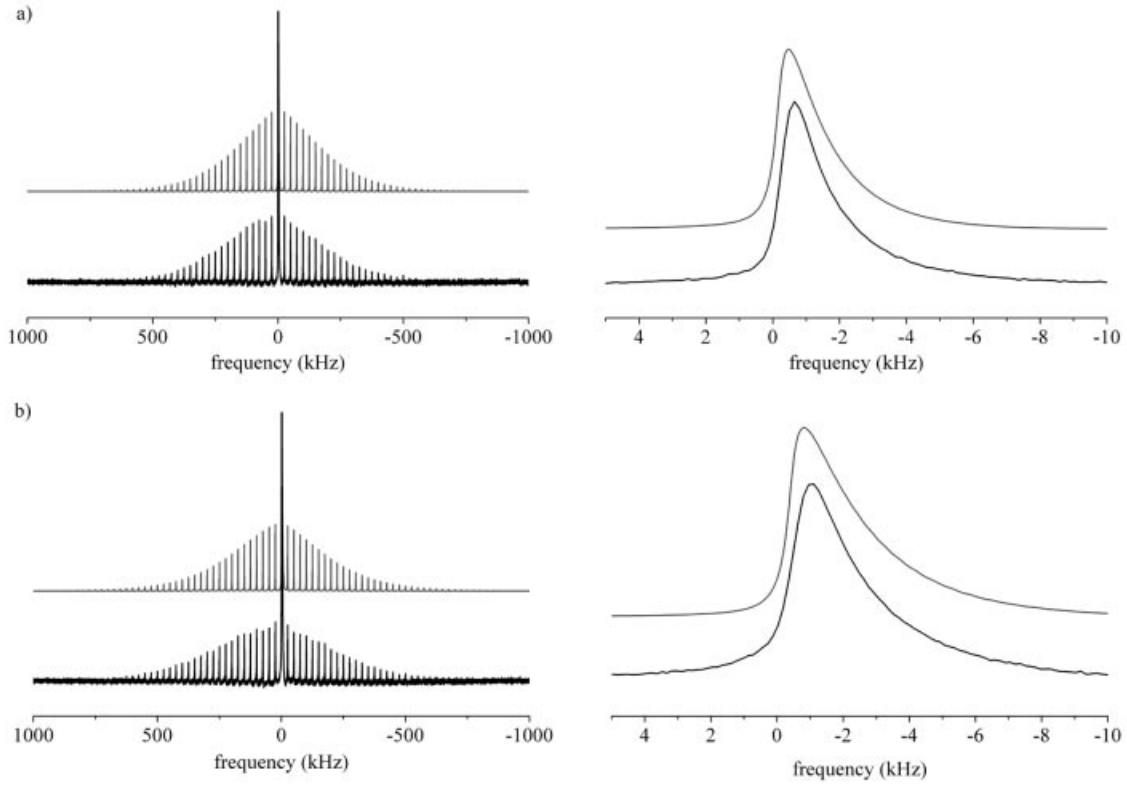


Figure 8. Experimental (bottom) and reconstructed (top) $^{27}$Al SATRAS spectra (left) and central transitions (right) for (a) $50CaF_2$–$15BaF_2$–$35AlF_3$, and (b) $35CaF_2$–$15BaF_2$–$50AlF_3$ glasses at 25 kHz. In the full SATRAS spectra the central transitions are truncated to improve the visiblity of the spinning sidebands.

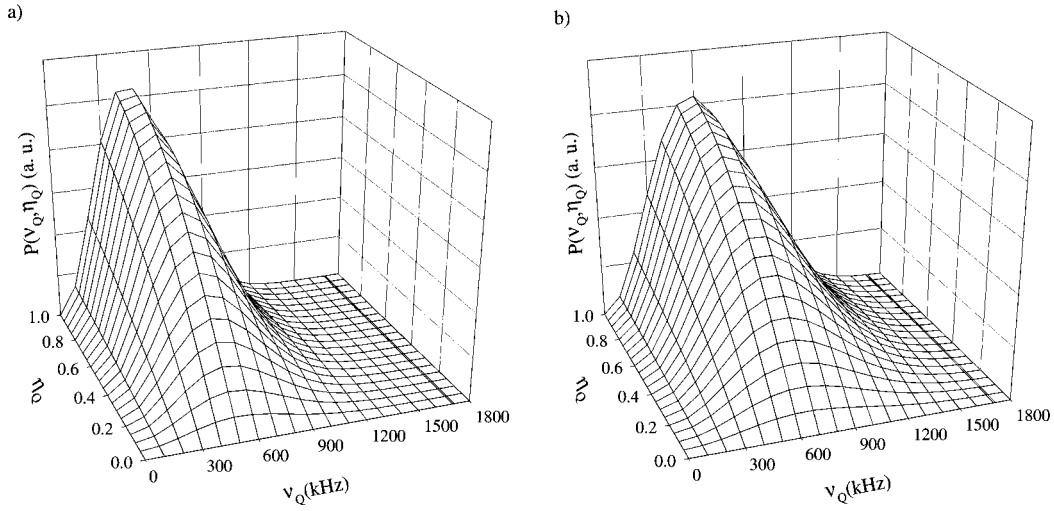


Figure 9. Quadrupolar parameter distributions, $P(\nu_Q, \eta_Q)$, for (a) $\sigma$ = 370 kHz and $d$ = 3; (b) $\sigma$ = 470 kHz and $d$ = 3.

## Discussion

For all the crystalline and glassy phases investigated, the isotropic chemical shift values are between –7 ppm and 1 ppm (Tables 1 and 2), which are typical $\delta_{iso}$ values for $Al^{3+}$ ions in $AlF_6^{3-}$ octahedra. The $\eta_Q$ values deviate from zero, which indicates that the $AlF_6^{3-}$ octahedra are rhombically distorted, in agreement with the crystal data.

For α- and β-$CaAlF_5$ the $\nu_Q$ values are equal to 1580 kHz and 1530 kHz, respectively. Both structures are built up by *trans*-connected $AlF_6^{3-}$ octahedra. The structures of α-, β- and γ-$BaAlF_5$, and $Ba_3Al_2F_{12}$ contain $AlF_6^{3-}$ octahedra that are *cis*-connected at the corners, and the $\nu_Q$ values are between 550 kHz and 1250 kHz. Isolated octahedra are encountered only in $Ca_2AlF_7$, $Ba_3AlF_9$-Ib, β-$Ba_3AlF_9$ and α-

  

$BaCaAlF_7$, and the $\nu_Q$ values range from 75 kHz to 510 kHz (Table 1).

It is well known that a bond involving a shared F ligand is usually longer than one involving an unshared F ligand. For example, in α-$CaAlF_5$[35] the Al-shared F distance is equal to 1.873 Å, and the Al-unshared F distances are equal to 1.806 Å and 1.749 Å. For *trans*-connected octahedron structures these bonds lie in opposite directions and the experimental $\nu_Q$ values are the highest of those measured. The charge distribution is expanded along the longest bond axis, which may correspond to the main *z* axis of the EFG. In the case of the *cis*-connected octahedron structures, the angle formed by the two longest bonds is around 90°, and the experimental $\nu_Q$ values are smaller than those measured for the *trans*-connected structures. We may assume that in this case the charge distribution is expanded along a direction that bisects the two longest bonds; as a result, the axial character of the charge distribution around the aluminium atom in the *cis*-connected octahedra is less pronounced than in the case of the *trans*-connected octahedra. For isolated octahedra the experimental $\nu_Q$ values are the smallest values measured, so in this case the axial character of the charge distributions around the Al atoms is even less pronounced than in the two previous cases, which may be related to smaller differences between the Al–F bond lengths. From these results it appears that the $\nu_Q$ value, which is related to the largest component of the EFG, could account for the way in which the $AlF_6^{3-}$ octahedra are connected i.e. in a *trans*, *cis* or isolated manner.

The main results for the glassy phases are as follows: (i) the low $\delta_{iso}$ values indicate that the $Al^{3+}$ ions are six-fold coordinated; (ii) the quadrupolar parameter distributions have $\nu_Q$ values that are usually encountered in cases where *cis*-connected and isolated octahedra are present in crystalline phases; (iii) the width of the $\nu_Q$ distribution increases with increasing $AlF_3$ content. In a previous $^{19}F$ NMR study[34] the $\beta$ parameter, which gives the mean number of F atoms per octahedron, was found to equal 6 for the glass with 35% $AlF_3$ content. Therefore, it can be stated that the glassy structure contains isolated $AlF_6^{3-}$ octahedra only. The reconstruction of the corresponding SATRAS spectrum indicates that most of the $\nu_Q$ values are between 100 kHz and 900 kHz (Figure 9). It is noticeable that these values appear to be slightly larger than for the crystalline phases containing isolated $AlF_6^{3-}$ octahedra (Table 1). Conversely, for the glass with a 50% $AlF_3$ content, the $\beta$ parameter was found to equal 5, which indicates that, on average, all octahedra are connected at two corners. The $\nu_Q$ range is enlarged to 1200 kHz, and accordingly the maximum $\nu_Q$ value increases from ca. 450 kHz to ca. 600 kHz (Figure 9). This increase in the $\nu_Q$ values with increasing $AlF_3$ content is in agreement with the previous observation based on the crystalline structures. The quadrupolar parameter distributions determined for the intermediate compositions confirm that the ratio of connected octahedra increases along with the $AlF_3$ content. In the glassy samples most of the $\nu_Q$ values range from 100 kHz to 1200 kHz, so we may infer that the *cis* connection is the favoured mode of bonding as far as the octahedra are connected. However, since low $\nu_Q$ values are observed for all the glasses investigated, we may infer that they contain isolated octahedra ($\beta$ = 6). For the glass comprising 50% $AlF_3$, we should assume the presence of ramified chains ($\beta < 5$) rather than infinite chains ($\beta$ = 5), as previously deduced from our $^{19}F$ NMR study.[34]

## Conclusion

$^{27}Al$ SATRAS and 3Q-MAS spectra (for compounds with several Al sites) were recorded for eight crystalline compounds from binary $CaF_2$–$AlF_3$ and $BaF_2$–$AlF_3$ and ternary $BaF_2$–$CaF_2$–$AlF_3$ systems, and four glass compositions with different $CaF_2/BaF_2/AlF_3$ contents.

For the crystalline phases the reconstruction of the spectra leads to the precise determination of the NMR parameters ($\delta_{iso}$, $\nu_Q$ and $\eta_Q$). For the glassy phases the $^{27}Al$ SATRAS spectra have been reconstructed using Czjzek distributions, and the relevant parameters ($\delta_{iso}$ and $\sigma$) were determined.

In agreement with the crystalline and glassy structures, the experimental $\delta_{iso}$ values are typical for $Al^{3+}$ ions in $AlF_6^{3-}$ octahedra. The measured $\eta_Q$ values are not equal to zero, which indicates that the $AlF_6^{3-}$ octahedra are rhombically distorted. It should be noted that despite of the precise determination of the quadrupolar parameters, it was impossible to relate these values to the two Al sites in β- and γ-$BaAlF_5$ both of which have the same multiplicity.

The most interesting finding from this study is the dependence of the quadrupolar frequency on the $AlF_6^{3-}$ octahedron connectivity. For crystalline phases the $\nu_Q$ values are measured between 75 kHz and 510 kHz for structures built up from isolated $AlF_6^{3-}$ octahedra, between 560 kHz and 1250 kHz for structures built up from isolated chains of *cis*-connected $AlF_6^{3-}$ octahedra, and between 1530 kHz and 1580 kHz for structures built up from isolated chains of *trans*-connected $AlF_6^{3-}$ octahedra. In the glassy phases the maximum of the quadrupolar frequency distribution is shifted towards larger values, and its width increases with increasing $AlF_3$ content and therefore the number of connected octahedra. The range of the $\nu_Q$ values seems to indicate that when the octahedra are connected, the most encountered connections are of the *cis* type.

In order to gain a deeper understanding of the dependence of the $\nu_Q$ values on the $AlF_6^{3-}$octahedron network connectivity, ab initio EFG calculations of $^{27}Al$ in crystalline phases are in progress. These calculations will provide important structural information about the sign and the orientation of the EFG tensors with respect to the crystallographic axes. They should also enable us to relate the quadrupolar parameters to the Al sites in the case of multi-site compounds such as β- and γ-$BaAlF_5$.

## Experimental Section

**Sample Preparation:** Owing to the fact that the fluoride compounds are moisture-sensitive, all weighting, mixing and grinding opera-

  

tions were done under anhydrous nitrogen. Before heating, the mixtures were introduced into Pt tubes sealed under anhydrous conditions. The crystalline compounds were synthesized as powders by solid-state reaction of mixtures containing the fluorides $AlF_3$, $CaF_2$ and/or $BaF_2$; the synthesis conditions are detailed in ref.[33] The purity and crystallinity of the phases were monitored by powder X-ray diffraction analysis. The glassy phases were obtained by heating $BaF_2/CaF_2/AlF_3$ mixtures at 1000 °C over a period of 1 h, followed by quenching in cold water. The glass formation was checked by powder X-ray diffraction (the XRD spectra should be featureless). Information regarding the glass formation area is reported in ref.[34]

**High-Resolution Solid-State NMR:** The high-resolution $^{27}$Al NMR spectra were recorded at 78.2 MHz with a Bruker Avance 300 spectrometer. CP MAS probes with 4 mm and 2.5 mm rotors were used for low and high spinning speeds, respectively. The $^{27}$Al isotropic chemical shifts were referenced to a 1 M aqueous solution of $Al(NO_3)_3$. $^{27}$Al SATRAS spectra[1,2] were recorded for all samples. To ensure a linear response regime[52] we chose the pulse duration and the RF field strength to equal 1 μs and 26 kHz, respectively. The recycle delay was set at 1 s. Under these experimental conditions the relative peak intensities are quantitative. The reconstructions of these spectra were achieved using an in-house FORTRAN 95 code based on the theoretical treatment developed by Skibsted et al.,[1,53] and including a correction for the second-order frequency shift, the formula for which is given in ref.[54,26] The adjustable parameters for the crystalline compounds are the quadrupolar frequency, $\nu_Q$, the asymmetry parameter, $\eta_Q$, and the chemical shift tensor, $\delta$. For the glassy phases the SATRAS spectra were reconstructed using the distributions of the quadrupolar parameters ($\nu_Q$, $\eta_Q$) implemented in the FORTRAN 95 code. For the crystalline multi-site compounds and for the glasses MQ-MAS experiments[3] were also carried out using a high-speed CP MAS probe with a 2.5 mm rotor. In the present case 3Q-MAS experiments were performed using a *z*-filter sequence without decoupling. The magnetic field strength was 188 kHz for the two hard pulses, and 8 kHz for the soft pulse. The pulse lengths were equal to 2.7 μs, 0.95 μs, and 10 μs, respectively. A two-dimensional Fourier transformation followed by a shearing[55] transformation gave 2D absorption spectra. For crystalline multi-site compounds an estimation of the quadrupolar parameters and chemical shift values of each contribution was obtained by simulating the corresponding *F1* slices with the DMFit[56] software.

## Acknowledgments

We thank A. Le Bail and A.-M. Mercier, from the Laboratoire des Oxydes et Fluorures, CNRS UMR 6010, who kindly supplied us with the three $BaAlF_5$ structural forms.

[1] J. Skibsted, N. C. Nielsen, H. J. Bildsoe, H. J. Jakobsen, *J. Magn. Reson.* **1991**, *95*, 88–117.
[2] C. Jäger in *Solid State NMR II* (Ed.: B. Blümich), Springer-Verlag, Berlin, **1994**, pp. 133–170.
[3] L. Frydman, J. S. Harwood, *J. Am. Chem. Soc.* **1995**, *117*, 5367–5368.
[4] P. Faucon, J.-C. Petit, T. Charpentier, J. F. Jacquinot, F. Adenot, *J. Am. Ceram. Soc.* **1999**, *82*, 1307–1312.
[5] L. B. Alemany, R. L. Callender, A. R. Barron, S. Steuernagel, D. Iuga, A. P. M. Kentgens, *J. Phys. Chem. B* **2000**, *104*, 11612–11616.
[6] T. Vosegaard, D. Massiot, P. J. Grandinetti, *Chem. Phys. Lett.* **2000**, *326*, 454–460.
[7] C. Gervais, K. J. D. MacKenzie, M. E. Smith, *Magn. Reson. Chem.* **2001**, *39*, 23–28.
[8] S. Ding, C. A. McDowell, *Chem. Phys. Lett.* **2001**, *333*, 413–418.
[9] O. H. Han, C.-S. Kim, S. B. Hong, *Angew. Chem.* **2002**, *114*, 487–490.
[10] M. Capron, F. Fayon, J. Coutures, D. Massiot, A. Douy, *J. Solid State Chem.* **2002**, *169*, 53–59.
[11] J.-P. Amoureux, C. Huguenard, F. Engelke, F. Taulelle, *Chem. Phys. Lett.* **2002**, *356*, 497–504.
[12] U. G. Nielsen, A. Boisen, M. Brorson, C. J. H. Jacobsen, H. J. Jakobsen, J. Skibsted, *Inorg. Chem.* **2002**, *41*, 6432–6439.
[13] M. Capron, F. Fayon, D. Massiot, A. Douy, *Chem. Mater.* **2003**, *15*, 575–579.
[14] S. Ganapathy, K. U. Gore, R. Kumar, J.-P. Amoureux, *Solid State Nucl. Magn. Reson.* **2003**, *24*, 184–195.
[15] G. Silly, C. Legein, J.-Y. Buzaré, F. Calvayrac, *Solid State Nucl. Magn. Reson.* **2004**, *25*, 241–251.
[16] R. Stösser, G. Scholz, J.-Y. Buzaré, G. Silly, M. Nofz, D. Schultze, *J. Am. Ceram. Soc.* **2005**, *88*, 2913–2922.
[17] J. Jiao, J. Kanellopoulos, W. Wang, S. S. Ray, H. Foerster, D. Freude, M. Hunger, *Phys. Chem. Chem. Phys.* **2005**, *7*, 3221–3226.
[18] M. Body, G. Silly, C. Legein, J.-Y. Buzaré, *J. Solid State Chem.* **2005**, *178*, 3655–3661.
[19] M. Body, G. Silly, C. Legein, J.-Y. Buzaré, *Chem. Phys. Lett.* **2006**, *424*, 321–326.
[20] C. Martineau, M. Body, C. Legein, G. Silly, J.-Y. Buzaré, F. Fayon, *Inorg. Chem.* **2006**, *45*, 10215–10223.
[21] D. Iuga, S. Simon, E. De Boer, A. P. M. Kentgens, *J. Phys. Chem. B* **1999**, *103*, 7591–7598.
[22] V. Montouillot, D. Massiot, A. Douy, J. P. Coutures, *J. Am. Ceram. Soc.* **1999**, *82*, 3299–3304.
[23] F. Angelli, T. Charpentier, P. Faucon, J.-C. Petit, *J. Phys. Chem. B* **1999**, *103*, 10356–10364.
[24] J. A. van Bokhoven, A. L. Roest, D. C. Koningsberger, J. T. Miller, G. H. Nachtegaal, A. P. M. Kentgens, *J. Phys. Chem. B* **2000**, *104*, 6743–6754.
[25] P. J. Chupas, M. F. Ciraolo, J. C. Hanson, C. P. Grey, *J. Am. Chem. Soc.* **2001**, *123*, 1694–1702.
[26] G. Scholz, R. Stösser, J. Klein, J.-Y. Buzaré, G. Silly, Y. Laligant, B. Ziemer, *J. Phys.: Condens. Matter* **2002**, *14*, 2101–2117.
[27] M. Fechtelkord, H. Behrens, F. Holtz, J. L. Bretherton, C. A. Fyfe, L. A. Groat, M. Raudsepp, *Am. Mineral.* **2003**, *88*, 1046–1054.
[28] D. R. Neuville, L. Cormier, D. Massiot, *Geochim. Cosmochim. Acta* **2004**, *68*, 5071–5079.
[29] D. Iuga, C. Morais, Z. Gan, D. R. Neuville, L. Cormier, D. Massiot, *J. Am. Chem. Soc.* **2005**, *127*, 11540–11541.
[30] F. Prescuitti, D. Capitani, A. Sgamellotti, B. G. Brunetti, F. Costantino, S. Viel, A. Segre, *J. Phys. Chem. B* **2005**, *109*, 22147–22158.
[31] A. de Kozak, M. Samouël, J. Renaudin, G. Férey, *Z. Anorg. Allg. Chem.* **1992**, *613*, 98–104.
[32] M. Weil, E. Zobetz, F. Werner, F. Kubel, *Solid State Sci.* **2001**, *3*, 441–453.
[33] M. Body, G. Silly, C. Legein, J.-Y. Buzaré, *Inorg. Chem.* **2004**, *43*, 2474–2485.
[34] M. Body, C. Legein, G. Silly, J.-Y. Buzaré, to be published in *J. Non-Cryst. Solids.*
[35] A. Hémon, G. Courbion, *Acta Crystallogr., Sect. C* **1991**, *47*, 1302–1303.
[36] R. Domesle, R. Hoppe, *Z. Anorg. Allg. Chem.* **1982**, *495*, 16–26.
[37] A. Le Bail, G. Férey, A.-M. Mercier, A. de Kozak, M. Samouël, *J. Solid State Chem.* **1990**, *89*, 282–291.
[38] S. Sakida, M. Shojiya, Y. Kawamoto, *J. Fluorine Chem.* **2000**, *106*, 127–131.
[39] R. Domesle, R. Hoppe, *Z. Anorg. Allg. Chem.* **1982**, *195*, 27–38.
[40] V. Kaiser, D. Babel, *Z. Anorg. Allg. Chem.* **2004**, *630*, 794–798.
[41] R. Domesle, R. Hoppe, *Z. Kristallogr.* **1980**, *153*, 317–328.

  

[42] J. Renaudin, G. Férey, A. de Kozak, M. Samouël, *Eur. J. Solid State Inorg. Chem.* **1991**, *28*, 373–381.
[43] A. Le Bail, *J. Solid State Chem.* **1993**, *103*, 287–291.
[44] F. Werner, M. Weil, *Acta Crystallogr., Sect. E* **2003**, *59*, i17–i19.
[45] J. C. C. Chan, H. Eckert, *J. Non-Cryst. Solids* **2001**, *284*, 16–21.
[46] G. Czjzek, J. Fink, F. Götz, H. Schmidt, J. M. D. Coey, J.-P. Rebouillat, A. Liénard, *Phys. Rev. B* **1981**, *23*, 2513–2530.
[47] G. Czjzek, *Phys. Rev. B* **1982**, *25*, 4908–4910.
[48] G. Le Caër, R. A. Brand, *J. Phys.: Condens. Matter* **1998**, *10*, 10715–10774.
[49] B. Bureau, G. Silly, J.-Y. Buzaré, C. Legein, D. Massiot, *Solid State Nucl. Magn. Reson.* **1999**, *15*, 129–138.
[50] B. Bureau, H. Guérault, G. Silly, J.-Y. Buzaré, J.-M. Grenèche, *J. Phys.: Condens. Matter* **1999**, *11*, L423–L431.
[51] B. Bureau, G. Silly, J.-Y. Buzaré, B. Boulard, C. Legein, *J. Phys.: Condens. Matter* **2000**, *12*, 5775–5788.
[52] M. E. Smith, E. R. H. van Eck, *Prog. Nucl. Magn. Reson. Spectrosc.* **1999**, *34*, 159–201.
[53] J. Skibsted, N. C. Nielsen, H. Bildsoe, H. J. Jakobsen, *Chem. Phys. Lett.* **1992**, *188*, 405–412.
[54] S. Ding, C. A. McDowell, *Chem. Phys. Lett.* **2001**, *333*, 413–418.
[55] R. Ernst, G. Bodenhausen, A. Wokaun, *Principles of Nuclear Magnetic Resonance in One and Two Dimensions*, Oxford University Press, New York, **1987**.
[56] D. Massiot, F. Fayon, M. Capron, I. King, S. Le Calvé, B. Alonso, J.-O. Durand, B. Bujoli, Z. Gan, G. Hoatson, *Magn. Reson. Chem.* **2002**, *40*, 70–76.

Received: December 5, 2006
Published Online: March 28, 2007

  